

Role of RDS and Rhodopsin in *Cngb1*-Related Retinal Degeneration

Dibyendu Chakraborty,¹ Shannon M. Conley,¹ Steven J. Pittler,² and Muna I. Naash³

¹Department of Cell Biology, University of Oklahoma Health Sciences Center, Oklahoma City, Oklahoma, United States

²Department of Vision Sciences, School of Optometry, University of Alabama at Birmingham, Birmingham, Alabama, United States

³Department of Biomedical Engineering, University of Houston, Houston, Texas, United States

Correspondence: Muna I. Naash, Department of Biomedical Engineering, University of Houston, 3517 Cullen Boulevard, Room 2011, Houston, TX 77204-5060, USA; mnaash@central.uh.edu.

Submitted: October 27, 2015

Accepted: January 29, 2016

Citation: Chakraborty D, Conley SM, Pittler SJ, Naash MI. Role of RDS and rhodopsin in *Cngb1*-related retinal degeneration. *Invest Ophthalmol Vis Sci.* 2016;57:787–797. DOI:10.1167/iov.15-18516

PURPOSE. Rod photoreceptor outer segment (OS) morphogenesis, structural integrity, and proper signal transduction rely on critical proteins found in the different OS membrane domains (e.g., plasma, disc, and disc rim membrane). Among these key elements are retinal degeneration slow (RDS, also known as peripherin-2), rhodopsin, and the beta subunit of the cyclic nucleotide gated channel (CNGB1a), which have been found to interact in a complex. The purpose of this study was to evaluate the potential interplay between these three proteins by examining retinal disease phenotypes in animal models expressing varying amounts of CNGB1a, rhodopsin, and RDS.

METHODS. Outer segment trafficking, retinal function, and photoreceptor structure were evaluated using knockout mouse lines.

RESULTS. Eliminating *Cngb1* and reducing RDS leads to additive defects in RDS expression levels and rod electroretinogram (ERG) function, (e.g., *Cngb1*^{-/-}/*rds*^{+/-} versus *rds*^{+/-} or *Cngb1*^{-/-}) but not to additive defects in rod ultrastructure. These additive effects also manifested in cone function: Photopic ERG responses were significantly lower in the *Cngb1*^{-/-}/*rds*^{+/-} versus *rds*^{+/-} or *Cngb1*^{-/-}, suggesting that eliminating *Cngb1* can accelerate the cone degeneration that usually presents later in the *rds*^{+/-}. This was not the case with rhodopsin; reducing rhodopsin levels in concert with eliminating CNGB1a did not lead to phenotypes more severe than those observed in the *Cngb1* knockout alone.

CONCLUSIONS. These data support a role for RDS as the core component of a multiprotein plasma membrane-rim-disc complex that has both a structural role in photoreceptor OS formation and maintenance and a functional role in orienting proteins for optimal signal transduction.

Keywords: RDS, *Cngb1*, rhodopsin, retina, tetraspanin, retinal degeneration

The rod outer segment (OS) contains a series of tightly packed membranous discs circumscribed by a rim region and enclosed by the plasma membrane. Organization of this structure, and in particular the three membrane domains (the plasma, disc, and rim membranes), is critical for proper phototransduction and vision, and mutations in proteins responsible for organizing/forming this structure lead to inherited retinal degeneration. Here we evaluate the potential interplay and relative contributions of three of the proteins critical for the formation and function of the OS, namely, the visual pigment rhodopsin, the ion channel subunit CNGB1a (cyclic nucleotide gated channel B1a), and the structural protein RDS (retinal degeneration slow, also known as peripherin/rds or peripherin-2).

Mutations in rhodopsin cause autosomal dominant retinitis pigmentosa (ADRP) (<http://www.retina-international.org/files/sci-news/rhomut.htm> [in the public domain]).¹ Rhodopsin is the predominant component of the disc membrane,^{2,3} and in addition to its key role in phototransduction, it also has a structural role in forming and maintaining OSs.^{4,5} In the absence of rhodopsin (*Rho*^{-/-} mice), rod OSs are not elaborated, and rod function is not detectable by ERG.^{6,7} However, flattened membranous vesicles reminiscent of

nascent discs form inside small sacs of OS plasma membrane, suggesting aborted attempts at OS formation.^{7,8} Although rhodopsin is present in the OS in high quantities and is precisely arranged in structurally distinct arrays in the disc membrane, reduction in rhodopsin levels by ~50% is well tolerated; that is, *Rho*^{+/-} retinas exhibit well-formed OSs that are quite similar structurally and functionally to those found in wild type (WT).^{9,10} Rhodopsin-associated disease is typically dominantly inherited, with dominant-negative, rather than loss-of-function/haploinsufficiency mutations, underlying the majority of cases.

While rhodopsin is a principal disc component, RDS is a tetraspanin membrane protein exclusively localized to the rim region of the disc^{11,12} and is required for OS disc morphogenesis and stabilization. Mutations in the *RDS* gene are associated with ADRP as well as multiple classes of macular degeneration (<http://www.retina-international.org/files/sci-news/rdsmut.htm> [in the public domain]).^{13,14} Retinal degeneration slow function relies on the assembly of a variety of types of homo- and hetero-oligomeric complexes containing RDS and its homologue rod outer segment membrane protein-1 (ROM-1). The C-terminus of RDS promotes membrane fusion in vitro¹⁵ and can initiate membrane curvature,¹⁶ suggesting it may play a role in OS



TABLE. Antibodies Used for Immunofluorescence and Western Blotting

Antigen	Antibody	Species	Source	Refs.
RDS	RDS-CT	Rbt-PC	In-house	38, 39
RDS	mAB 2B7	Ms-MC	In-house	41, 42
ROM-1	ROM-1-CT	Rbt-PC	In-house	38, 39
ROM-1	mAB 2H5	Ms-MC	In-house	41, 42
Rhodopsin	mAB 1D4	Ms-MC	Robert Molday	43
CNGB1, GARP1, GARP2	mAB GARP-4B1	Ms-MC	Robert Molday	17
CNGA1	mAB 1D1	Ms-MC	Robert Molday	
S-opsin	OPN1SW, N-20	Gt-PC	Santa Cruz Biotechnology, (Santa Cruz, CA, USA) cat no. sc-14363	
M-opsin	Opsin 1, medium wave	Rbt-PC	Novus Biologicals, (Littleton, CO, USA) cat no. 110-74730	

Rbt-PC, rabbit polyclonal; Ms-MC, mouse monoclonal; Gt-PC, goat polyclonal.

formation. Retinal degeneration slow also is known to interact with several other proteins, often through interactions mediated by the C-terminal. One notable binding partner of RDS is the CNGB1a channel subunit, which we further discuss below.^{17,18} More recently, using in vitro analyses, a direct binding of RDS to rhodopsin has been reported.¹⁹ In the *rds*^{-/-} (actually a naturally occurring null allele [*Prpfb*^{2rds/rds}], here referred to as *rds*^{-/-} to maintain continuity with previous work) OSs fail to form; the cells instead terminate with the connecting cilia.^{8,20} The *rds*^{-/-} retina exhibits negligible phototransduction activity, and subsequently degenerates.²⁰⁻²² In contrast to rhodopsin, lack of a single RDS allele (*rds*^{+/-}) results in severe abnormalities in OS structure and a reduction in rod function²³; and consistent with this observation, many RDS ADRP mutations cause disease in patients due to haploinsufficiency.^{23,24}

The rod CNG channel consists of three alpha subunits (CNGA1) and one longer beta subunit (CNGB1a).²⁵ It has an essential role in the phototransduction signaling cascade, and many *CNGB1* mutations lead to ADRP.²⁶⁻³³ The N-terminal of CNGB1a contains a unique proline- and glutamic acid-rich N-terminal extension protein domain called GARP³⁴; and in addition to the membrane-bound channel (CNGB1a), two additional cytosolic splice variants called GARP1/2 are expressed from the *CNGB1* gene. Though the “free,” that is, nonmembrane-bound GARP isoforms are present throughout the OS,^{35,36} the beta subunit (CNGB1a) is present exclusively in the rod OS plasma membrane.

Retinal degeneration slow interactions with CNGB1a and GARP have been hypothesized to stabilize the alignment of OS disc rims with the plasma membrane or to bridge adjacent rims, again to maintain proper OS structure.^{17,18} This hypothesis is supported by the observation that, though CNGB1a is not a structural protein per se, in the *Cngb1*^{-/-} retina, OS disc alignment and sizing are abnormal.^{34,37} Additionally, as noted above, direct binding of RDS to rhodopsin has been shown, and mutations in the fourth transmembrane domain of RDS can interrupt this binding and lead to ADRP.¹⁹ Thus, it has been hypothesized that RDS serves as an organizing component of both adjacent membrane domains (i.e., rhodopsin in the disc membrane and CNGB1a in the plasma membrane) to form functional domains, optimized for efficient signal transduction and structural stability.¹⁹ Here, we evaluate the potential interplay between these three proteins by examining retinal disease phenotypes in animal models expressing varying amounts of CNGB1a, rhodopsin, and RDS.

MATERIALS AND METHODS

Ethics Statement and Animal Care and Use

Animal use was approved by the Institutional Animal Care and Use Committees at the University of Oklahoma Health

Sciences Center, Oklahoma City, Oklahoma, and the University of Houston and conformed to the ARVO Statement for the Use of Animals in Ophthalmic and Vision Research. The *Cngb1*^{-/-} line, the *rds*^{-/-} line (originally obtained from Neeraj Agarwal currently at the National Eye Institute, Bethesda, MD, USA), and the *Rbo*^{-/-} line (originally obtained from Janice Lem, Tufts University, Boston, MA, USA) have been described previously.^{7,22,34} *Cngb1*^{-/-} mice on the *rds*^{+/-}, *rds*^{-/-}, *Rbo*^{+/-}, and *Rbo*^{-/-} backgrounds were generated in our facility. Wild-type (i.e., *Cngb1*^{+/+}/*rds*^{+/-}/*Rbo*^{+/-}), *rds*^{+/-}, *rds*^{-/-}, *Rbo*^{+/-}, and *Rbo*^{-/-} littermates were used from our colony as controls. All animals were maintained in cyclic light (12 hours light, 12 hours dark, ~30 lux) and fed standard lab chow.

Immunofluorescence Labeling and Protein Chemistry

Western blot and velocity sedimentation were performed as described previously.^{38,39} Experiments were repeated three to seven times, and densitometry was done using the Image Lab Software (Bio-Rad, Temecula, CA, USA). Eyes for immunofluorescence were harvested, fixed, sectioned, and immunolabeled as previously described.^{38,40} Primary antibodies are described in the Table,^{38,39,41-43} and anti-mouse, anti-rabbit, or anti-goat AlexaFluor conjugated secondary antibodies (Life Technologies, Grand Island, NY, USA) were used. Images were captured on an Olympus BX-62 microscope (Center Valley, PA, USA) equipped with a spinning disc confocal unit and analyzed as described previously.^{41,44}

Light and Transmission Electron Microscopy

Tissue collection, processing, and plastic embedding and transmission electron microscopy (TEM) have been described previously.^{45,46} Light microscopy images were captured at $\times 40$ using a Zeiss (Peabody, MA, USA) universal microscope. To evaluate outer nuclear layer (ONL) and OS layer thickness, images were captured from central superior and inferior regions containing the optic nerve head, and at least three retinal sections from two to four eyes/genotype were used. Layer thickness was measured using Adobe Photoshop CS5 (Adobe Systems, Inc., San Jose, CA, USA).

Electroretinography

Electroretinography (ERG) was performed as previously described.^{45,46} Assessment of rod photoreceptor function (scotopic ERG) was performed on dark-adapted animals with a strobe flash stimulus of 157 cd-s/m² intensity while photopic responses were recorded using a similar stimulus from light-adapted animals. At least five or six mice per genotype were analyzed.

Statistical Analysis

Graphs are presented as mean \pm SEM. Differences between genotypes were assessed by 1-way or 2-way ANOVA with Bonferroni's post hoc pairwise comparisons. $P < 0.05$ was considered significant ($P < 0.05$, $P < 0.01$, and $P < 0.001$).

RESULTS

Levels of Rhodopsin, RDS, and ROM-1 Are Altered by Co-elimination of CNGB1 and RDS/Rhodopsin

Previously we evaluated the interplay between RDS and rhodopsin in OS morphogenesis,⁸ and here we wanted to understand the effects of eliminating CNGB1 at the same time as either rhodopsin or RDS. We crossed the *Cngb1*^{-/-} line, which lacks all *Cngb1* gene products including CNGB1a and GARP1/2,³⁴ onto the *rds*^{+/-}, *rds*^{-/-}, *Rbo*^{+/-}, and *Rbo*^{-/-} backgrounds (which were all used as control lines for the purpose of comparison throughout the study). At postnatal day (P) 30 we assessed levels of rhodopsin, RDS, and ROM-1 by reducing SDS-PAGE/Western blot. Data are presented as percentage of WT after normalization to actin (a loading control) (Figs. 1A-C) and are plotted as means \pm SEM ($P < 0.05$, $P < 0.01$, and $P < 0.001$ by 1-way ANOVA with Bonferroni's post hoc comparison). Though rhodopsin levels were virtually normal in the *Cngb1*^{-/-} and the *rds*^{+/-} (Fig. 1A), they were reduced in *Cngb1*^{-/-}/*rds*^{+/-} to ~56% of levels in the *rds*^{+/-}. Rhodopsin levels in the *Cngb1*^{-/-}/*Rbo*^{+/-} were ~64% those of the *Rbo*^{+/-}. Levels of rhodopsin in the *rds*^{-/-} were reduced by 84% and were not further reduced by ablating *Cngb1*.

This more pronounced effect of *Cngb1* ablation in the *rds*^{+/-} compared to the *Rbo*^{+/-} continued when we examined RDS levels (Fig. 1B). In *Cngb1*^{-/-}/*rds*^{+/-} retinas, RDS levels were reduced to ~54% of those in the *rds*^{+/-} while RDS levels in *Cngb1*^{-/-}/*Rbo*^{+/-} remained at ~87% of those in the *Rbo*^{+/-}. Rod outer segment membrane protein-1 levels were not altered in either the *Cngb1*^{-/-}/*rds*^{+/-} versus the *rds*^{+/-} or the *Cngb1*^{-/-}/*Rbo*^{+/-} versus the *Rbo*^{+/-} (Fig. 1C). We also observed that RDS and ROM-1 are severely reduced by the coablation of *Cngb1* and rhodopsin (*Cngb1*^{-/-}/*Rbo*^{-/-} had RDS/ROM-1 levels that were 8.8% and 7.9% those of *Rbo*^{-/-}, respectively).

Cyclic nucleotide gated channel B1a is known to bind to RDS in the OS,^{17,18} and proper binding and complex assembly of RDS/ROM-1 are necessary for OS formation,³⁸ so we asked whether eliminating *Cngb1* altered RDS/ROM-1 oligomerization. Retinal extracts from WT and *Cngb1*^{-/-} animals were fractionated on 5% to 20% nonreducing sucrose gradients and then separated on reducing SDS-PAGE. In the WT retina, RDS is present as tetramers (fractions 6-8), octamers (fractions 4-5), and higher-order oligomers (fractions 1-3) while ROM-1 is detected only in tetrameric and octameric fractions. We did not observe significant alteration in RDS (Fig. 1D) or ROM-1 (Fig. 1E) complex formation in *Cngb1*^{-/-} retinas, suggesting that RDS/ROM-1 oligomerization is not tied to CNGB1.

Previously we observed that CNGB1a and GARP2 protein levels are reduced by ~50% in the *rds*^{+/-} and are undetectable in the *rds*^{-/-}.⁴⁷ When combined with our data here showing that RDS levels are decreased in the *Cngb1*^{-/-}/*rds*^{+/-} compared to the *rds*^{+/-}, these data suggest that stability of CNGB1a and RDS may be interrelated.

Trafficking of OS Protein Is Largely Unaffected by Removing *Cngb1*

Cyclic nucleotide gated channel B1a and RDS binding occurs during the OS targeting process prior to arrival in the OS,¹⁸ so

we next used immunofluorescence labeling to ask whether the targeting of RDS, ROM-1, rhodopsin, or CNGB1a/GARP1/2 is affected by co-elimination of *Cngb1*, rhodopsin, or *Rds*. Retinal degeneration slow and ROM-1 labeling was properly restricted to the OS layer in the WT, *Cngb1*^{-/-}, *rds*^{+/-}, *Cngb1*^{-/-}/*Rbo*^{+/-}, *Rbo*^{+/-}, and *Cngb1*^{-/-}/*Rbo*^{+/-} retinas (Fig. 2A, green). Similarly, rhodopsin localization is not affected in most of these genotypes; however, some accumulation of rhodopsin in the ONL is observed in the *Cngb1*^{-/-}/*Rbo*^{+/-} (Fig. 2A, red, arrow). In the *rds*^{-/-}, large amounts of rhodopsin accumulate in the inner segment and ONL,⁸ and this is recapitulated in the *Cngb1*^{-/-}/*rds*^{-/-} (Fig. 2B, red). In contrast, in the *Rbo*^{-/-} and *Cngb1*^{-/-}/*Rbo*^{-/-} retinas, the majority of RDS is not found in the inner segment, but is properly restricted to the distal tips of the photoreceptors, consistent with our previous observation showing that RDS and ROM-1 are found in the small nascent OSs of the *Rbo*^{-/-}.⁸ However, in the *Rbo*^{-/-} and *Cngb1*^{-/-}/*Rbo*^{-/-} retinas, some mild mislocalization of RDS (but not ROM-1) to the inner segment, ONL, and outer plexiform layer is seen (arrows, Fig. 2C). Combined, these data suggest that while rhodopsin is more susceptible to mislocalization than RDS, CNGB1 ablation has little to no effect on the OS targeting of RDS, ROM-1, or rhodopsin.

Conversely, to see whether reduction/elimination of RDS or rhodopsin affected CNGB1a/GARP1/2 targeting, we labeled with GARP-4B1, which recognizes all *Cngb1* gene products (Fig. 2D, red). In WT, *rds*^{+/-}, and *Rbo*^{+/-} retinas, CNGB1a/GARP1/2 properly localized to the OS layer. This observation was replicated in the *Rbo*^{-/-} retina; CNGB1a/GARP1/2 properly localized to the OS layer, even though the *Rbo*^{-/-} does not form fully elaborated OSs. In striking contrast, and consistent with our Western blot data,⁴⁷ in the absence of RDS (*rds*^{-/-}), CNGB1a and GARP1/2 are virtually undetectable in the retina. This decrease in *Cngb1* gene products in the absence of RDS is clearly not due to a requirement for proper OS formation, since the OSs in the *Rbo*^{-/-} retina, while more formed than in the *rds*^{-/-}, are still just tiny sacs of vesicle-containing membrane at the tip of the OS,⁸ yet the *Rbo*^{-/-} model still expresses CNGB1a/GARP1/2. Rather it suggests that the stability or transport of CNGB1a and/or GARP 1/2 are dependent directly on RDS or on the initiation/formation of OSs by RDS (which can be seen in nascent form even in the *Rbo*^{-/-}).

Elimination of CNGB1 Exacerbates OS Shortening When RDS Is Also Reduced

We next conducted histologic and morphometric analysis at P30 (Fig. 3A). As expected at early time points, ONL thickness is not changed in *rds*^{+/-} or *Rbo*^{+/-} versus WT (Figs. 3B, 3C). However, though the differences do not attain statistical significance, mean ONL thickness in the *Cngb1*^{-/-}, *Cngb1*^{-/-}/*rds*^{+/-}, and *Cngb1*^{-/-}/*Rbo*^{+/-} was decreased by 10% to 15% compared to their respective controls (WT, *rds*^{+/-}, and *Rbo*^{+/-}), suggesting that degeneration in the *Cngb1*^{-/-}^{34,48} starts earlier than that in the *rds*^{+/-} and *Rbo*^{+/-}. There is no difference in ONL thickness in *Rbo*^{-/-} versus *Cngb1*^{-/-}/*Rbo*^{-/-} or *rds*^{-/-} versus *Cngb1*^{-/-}/*rds*^{-/-}, suggesting that the photoreceptor degeneration in the *rds*^{-/-} and *Rbo*^{-/-} is not additive with that in *Cngb1*^{-/-}.

It was previously shown that OSs are shorter and more disorganized in the *Cngb1*^{-/-} and *rds*^{+/-} retinas compared to WT,^{23,34} and our data confirm this (Fig. 3C). Interestingly, this effect was additive: In the *Cngb1*^{-/-}/*rds*^{+/-}, mean OS length was 41% of WT, compared to 52% and 73% of WT for *rds*^{+/-} and *Cngb1*^{-/-}, respectively (Fig. 3C). As expected, at P30, OSs in the *Rbo*^{+/-} are similar to those in WT, but we do see OS shortening in the *Cngb1*^{-/-}/*Rbo*^{+/-} due to the absence of

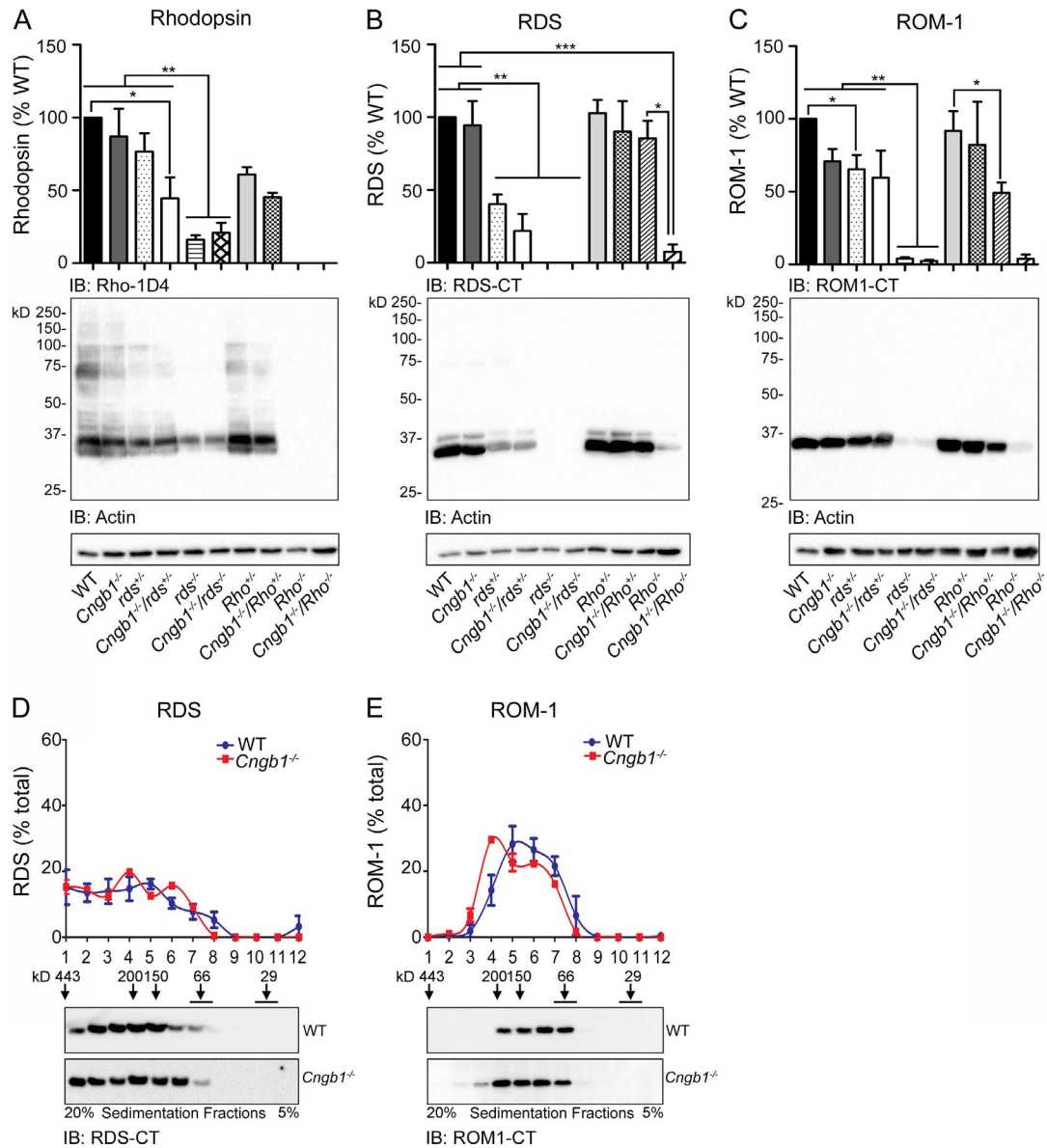


FIGURE 1. Levels of OS proteins are altered when *Cngb1* is absent. Retinal extracts were isolated from P30 eyes of the indicated genotypes and were analyzed by reducing SDS-PAGE/Western blot. The blots were probed with (A) mAb 1D4 against rhodopsin, (B) anti-RDS-CT, and (C) anti-ROM-1-CT. Blots were also labeled with actin as a loading control. Protein was quantified densitometrically, normalized to actin, and plotted as a percentage of WT (shown are means \pm SEM, * $P < 0.05$, ** $P < 0.01$, and *** $P < 0.001$ by 1-way ANOVA with Bonferroni's post hoc comparison). Measurements were performed in 3 to 7 retinas per genotype. Nonreducing sucrose gradient velocity sedimentation (D, E) was performed on P30 retinal extracts from WT and *Cngb1*^{-/-}. Fractions from gradients (1–12) were further separated by SDS-PAGE/reducing Western blot. Resulting blots were probed with anti-RDS-CT (D) and anti-ROM-1-CT (E). The relative percent of total RDS or ROM-1 in each fraction was assessed densitometrically and plotted as mean \pm SEM from 3 or 4 independent experiments.

CNGB1a; OSs in the *Rho*^{+/-} are 89% of WT, while those in the *Cngb1*^{-/-}/*Rho*^{+/-} are 59% of WT. Again, the effects of eliminating CNGB1a from the *rds*^{+/-} retina are more severe than in the *Rho*^{+/-} retina; for example, OSs in the *Cngb1*^{-/-}/*rds*^{+/-} are decreased to 56% of those in *Cngb1*^{-/-} ($P < 0.05$), while the OSs of the *Cngb1*^{-/-}/*Rho*^{+/-} are 81% of *Cngb1*^{-/-} (not significant).

Eliminating *Cngb1* Severely Affects Rod Function

We performed full-field scotopic ERG at P30 to evaluate rod function. Figure 4A shows representative waveforms, and maximum saturating a- and b-wave amplitudes are plotted in Figure 4B (mean \pm SEM, $P < 0.001$ by 1-way ANOVA with

Bonferroni's post hoc comparison). Our results for control animals (*Cngb1*^{-/-}, *rds*^{+/-}, and *rbo*^{+/-}) are consistent with previous publications^{8,34} (Fig. 4B). Again, elimination of *Cngb1* had a much more severe effect in the *rds*^{+/-} background than it did in the *Rho*^{+/-} background. Scotopic a-wave values in the *Cngb1*^{-/-}/*Rho*^{+/-} were not significantly reduced compared to the *Cngb1*^{-/-}, suggesting that all of the functional decrease in the *Cngb1*^{-/-}/*Rho*^{+/-} is due to the absence of *Cngb1*^{-/-}. In contrast, in the *Cngb1*^{-/-}/*rds*^{+/-}, scotopic ERG responses were severely reduced compared to both *Cngb1*^{-/-} and *rds*^{+/-} (Fig. 4B). This effect was seen in both the scotopic a- and b-waves, and scotopic a-waves in the *Cngb1*^{-/-}/*rds*^{+/-} were virtually undetectable. Scotopic ERG function is undetectable in the *rds*^{-/-} and *Rho*^{-/-} retina at P30, so we did not perform ERGs

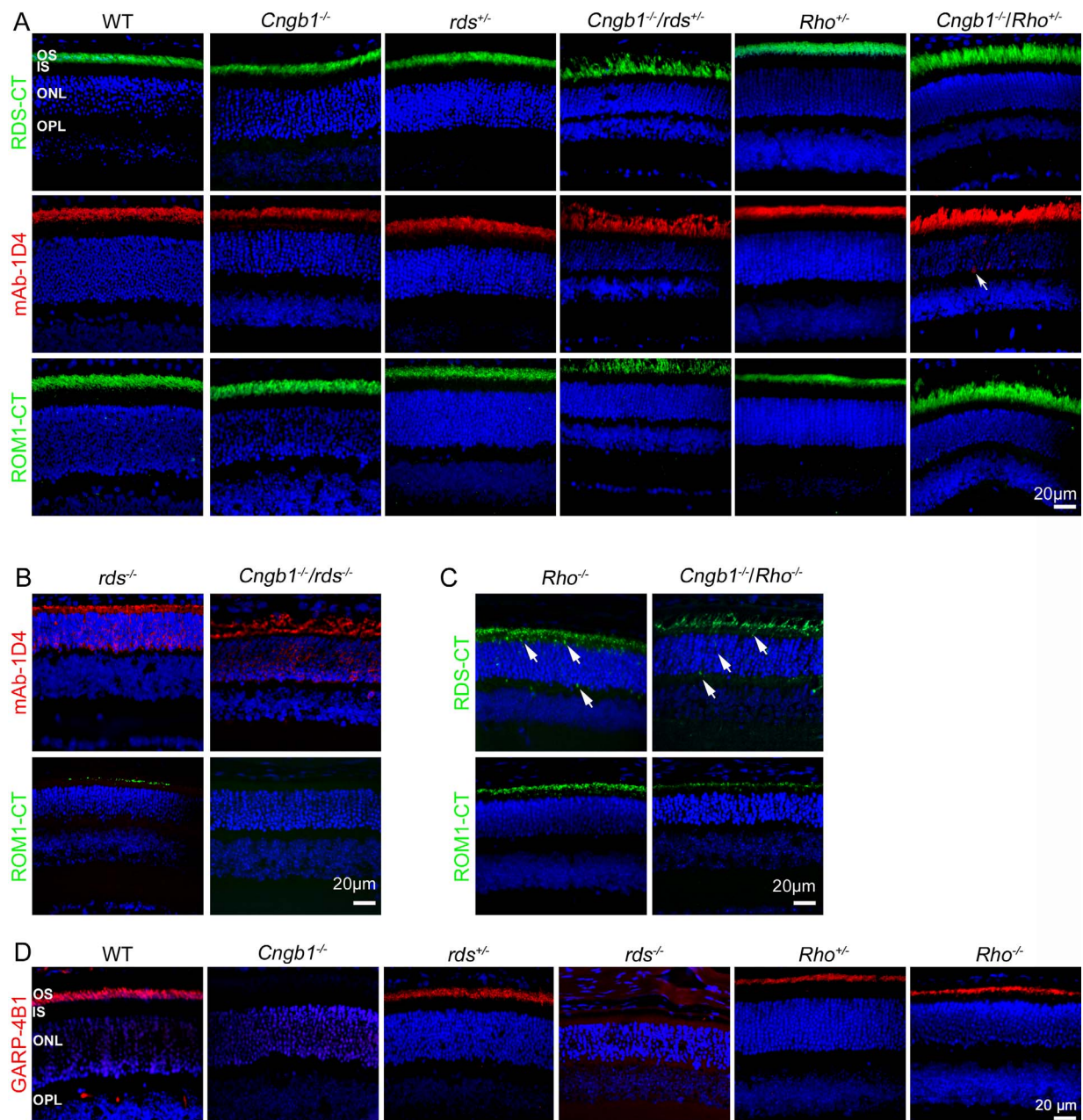


FIGURE 2. Eliminating *Cngb1* does not affect targeting of RDS or rhodopsin. Paraffin-embedded retinal sections from P30 animals of the indicated genotypes were labeled (A) with antibodies against RDS (RDS-CT, green), rhodopsin (mAb-1D4, red), or ROM-1 (ROM1-CT, green); (B) mAb 1D4 (red) or ROM1-CT (green); (C) RDS-CT or ROM1-CT (green), or (D) *Cngb1* gene products (GARP-4B1, red). In all cases nuclei were counterstained with DAPI (4',6-Diamidino-2-Phenylindole; blue). Arrows indicate accumulation of protein outside the OS. Scale bar: 20 μm. OS, outer segment; ONL, outer nuclear layer; IS, inner segment; OPL, outer plexiform layer.

on animals in those backgrounds. The additive ERG defect in the *Cngb1*^{-/-}/*rds*^{+/-} could be due to reductions in CNGA1; however, levels of CNGA1 in *Cngb1*^{-/-} are virtually undetectable,^{34,49} and this finding is recapitulated in *Cngb1*^{-/-}/*rds*^{+/-} (Supplementary Fig. S1). Thus while it is possible that further reduction in CNGA1 levels contributes to the additive defects seen in the *Cngb1*^{-/-}/*rds*^{+/-}, we cannot conclusively assess the possibility given that the levels of CNGA1 are below the limit of detection.

We conducted TEM to determine whether the severe effects of simultaneously eliminating *Cngb1* and reducing rhodopsin/*Rds* led to defects in OS ultrastructure (Fig. 4C with additional examples in Supplementary Fig. S2). The OS shortening we

quantified on the light microscopy level in the *Cngb1*^{-/-} is also evident by low-magnification EM (×3000, top, Fig. 4C). By high-magnification EM (×20,000, bottom, Fig. 4C), we find that the disc diameter and often the disc alignment are abnormal in the *Cngb1*^{-/-} retina. In some cases, new discs grew abnormally parallel to the plasma membrane (arrow, Fig. 4C, with additional examples in Supplementary Fig. S2), as previously reported.³⁴ Outer segments in the *rds*^{+/-} were characterized by abnormal disc size and the formation of highly dysmorphic whorl structures, but interestingly, this phenotype was not worsened in the *Cngb1*^{-/-}/*rds*^{+/-} retina. Outer segment structure in the *Cngb1*^{-/-}/*Rho*^{+/-} was worse than in the *Rho*^{+/-} (which is largely normal). The phenotype in the

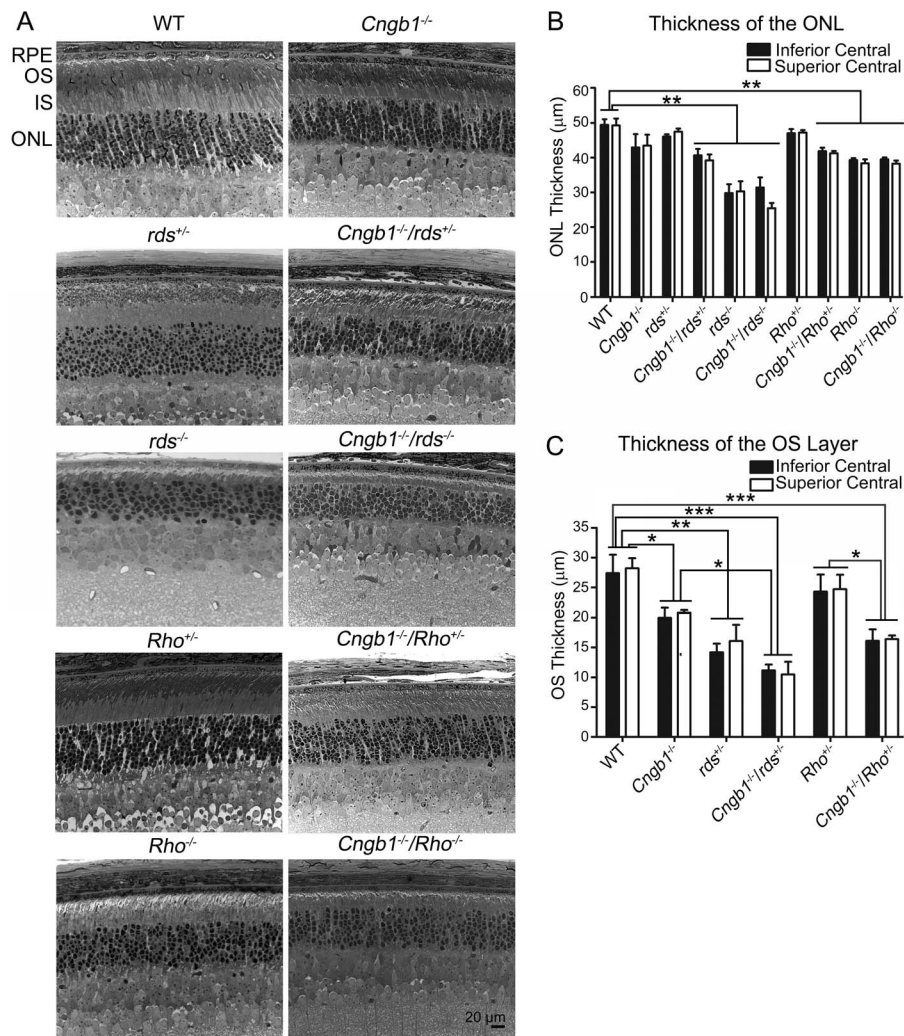


FIGURE 3. Outer segment length is reduced in the absence of *Cngb1*. Representative light micrographs (LM) were captured from plastic-embedded retinal sections harvested at P30 from the indicated genotypes. Scale bar for LM images is 20 μm . RPE, retinal pigment epithelium; OS, outer segment; IS, inner segment; ONL, outer nuclear layer. (B, C) Outer nuclear layer and OS layer thicknesses were measured in sections captured from the central superior and central inferior retina from 2 to 4 eyes per genotype. Plotted are means \pm SEM, * $P < 0.05$, ** $P < 0.01$, and *** $P < 0.001$ by 2-way ANOVA with Bonferroni's post hoc comparison.

Cngb1^{-/-}/*Rho*^{+/-} was of the same type seen in the *Cngb1*^{-/-}, namely, abnormalities in disc size and alignment but not whorl formation; however, the defects appeared to be more severe in the *Cngb1*^{-/-}/*Rho*^{+/-} compared to the *Cngb1*^{-/-}. The *rds*^{-/-} retina forms no OS at the tip of the connecting cilia (Fig. 5, CC marks connecting cilia), and the *Cngb1*^{-/-}/*rds*^{-/-} is not different from the *rds*^{-/-}. In contrast, the *Rho*^{-/-} forms well-characterized^{7,8} tiny nascent OSs (arrows, Fig. 5) distal to the connecting cilia with enclosed small flattened vesicular structures. Similar structures at the distal tip of the connecting cilium were seen in the *Cngb1*^{-/-}/*Rho*^{-/-} (arrows, Fig. 5).

Elimination of *Cngb1* Severely Affects Cone Function in the *rds*^{+/-} Retina

Though *Cngb1* is expressed only in rods, secondary cone loss can occur after rod defects. Therefore, we evaluated cone function in our models. Figure 6A shows representative photopic ERG waveforms while Figure 6B plots mean photopic b-wave amplitudes (mean \pm SEM, $P < 0.01$ by 1-way ANOVA with Bonferroni's post hoc comparison). Consistent with previous reports, at this time point significant decreases in

cone function are not detected in the *rds*^{+/-} or *Cngb1*^{-/-}.^{23,48} Likewise, no significant reductions in cone function were noticed in *Cngb1*^{-/-}/*Rho*^{+/-} versus *Rho*^{+/-} or WT. However, a striking $\sim 75\%$ reduction in cone function was observed in *Cngb1*^{-/-}/*rds*^{+/-} compared to WT, *rds*^{+/-}, and *Cngb1*^{-/-}. To identify whether this defect was associated with loss of cone cells, M-opsin-positive cones were counted in a region in the superior central retina while S-opsin-positive cones were counted in the inferior central portion of the retina (representative images in Fig. 6C; Fig. 6D shows mean \pm SEM). Consistent with the dramatic decrease in photopic ERG response in the *Cngb1*^{-/-}/*rds*^{+/-} compared to the *Cngb1*^{-/-} or the *rds*^{+/-}, we observed a 50% reduction in S-cones in the *Cngb1*^{-/-}/*rds*^{+/-} compared to *Cngb1*^{-/-}, *rds*^{+/-}, or WT controls ($P < 0.001$ by 1-way ANOVA).

DISCUSSION

In this study, our goal was to understand how RDS (a rim protein), rhodopsin (primarily a disc protein), and CNGB1a (a plasma membrane protein) are interrelated in their ability to

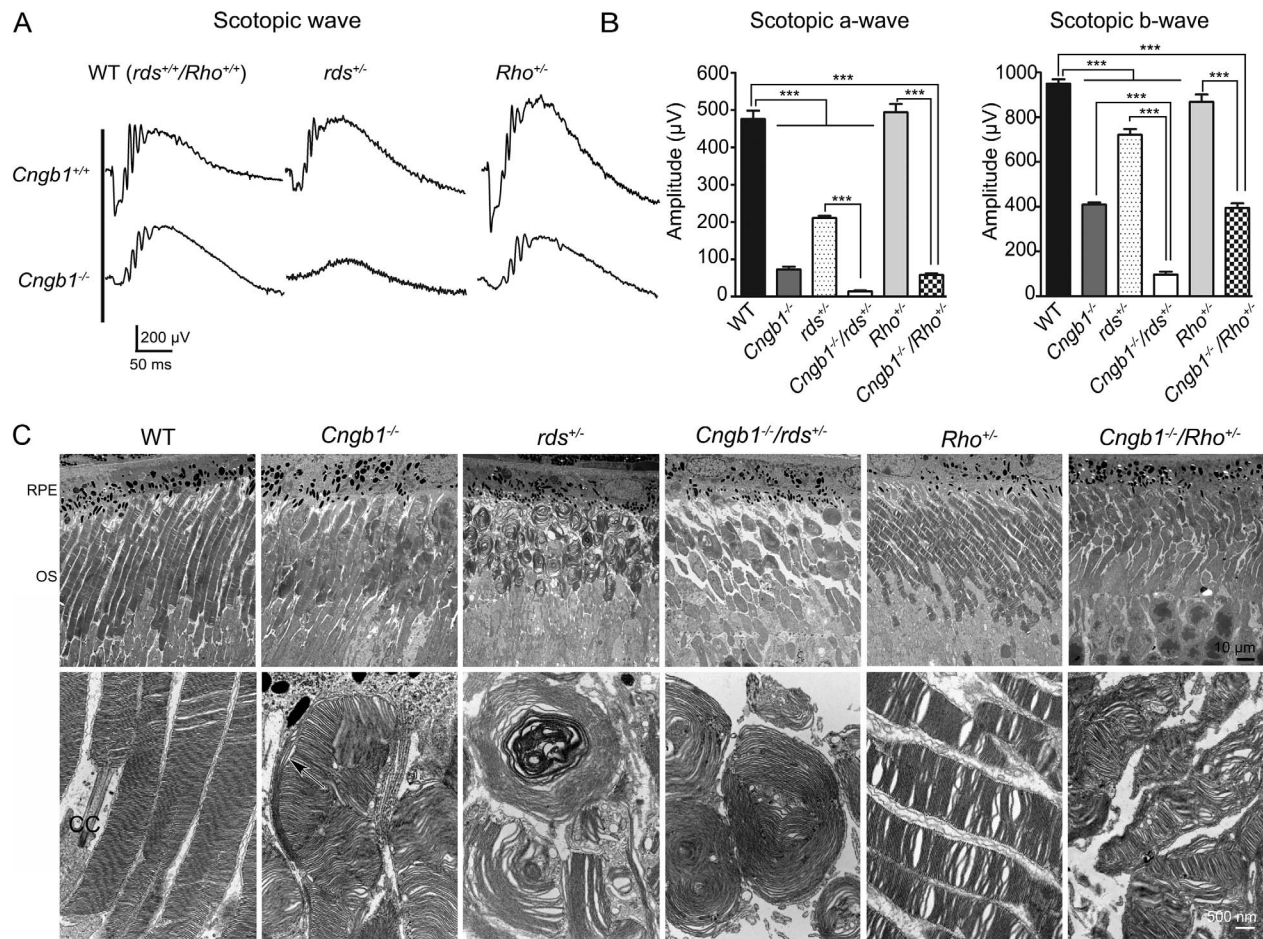


FIGURE 4. Absence of *Cngb1* significantly affects rod structure and function. Full-field scotopic ERG responses were obtained at P30. (A) Representative waveforms; (B) plots of mean amplitude \pm SEM from 4 to 7 mice per genotype ($*P < 0.05$, $**P < 0.01$, and $***P < 0.001$ by 1-way ANOVA with Bonferroni's post hoc comparison). (C) Representative TEM images of the photoreceptor-RPE interface at P30. Scale bars: 10 μ m for low-magnification EM images and 500 nm for higher-magnification EM images. RPE, retinal pigment epithelium; OS, outer segment; CC, connecting cilium.

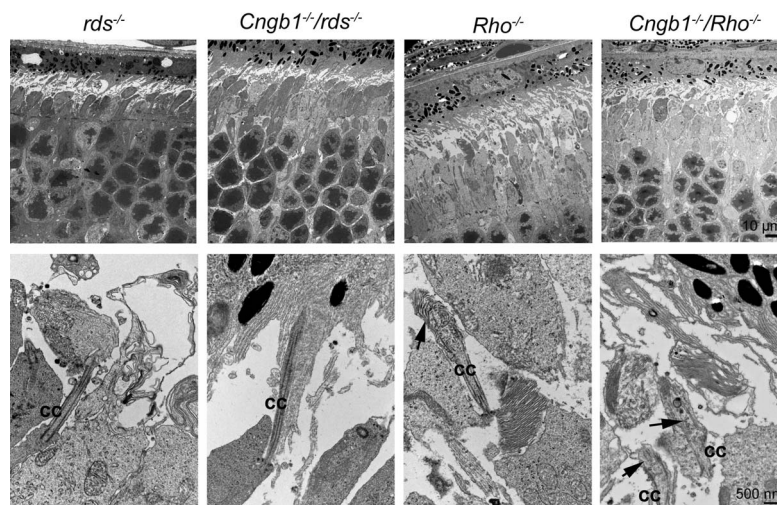


FIGURE 5. Outer segment ultrastructure in the *rds*^{-/-} and *Rho*^{-/-} is not affected by the ablation of CNGB1. Shown are representative TEM images captured from the indicated genotypes at P30. CC, connecting cilium. Arrows indicate nascent OS structures formed in retinas of animals on the *Rho*^{-/-} background. Scale bars: 10 μ m for low-magnification EM images (top) and 500 nm for higher-magnification EM images (bottom).

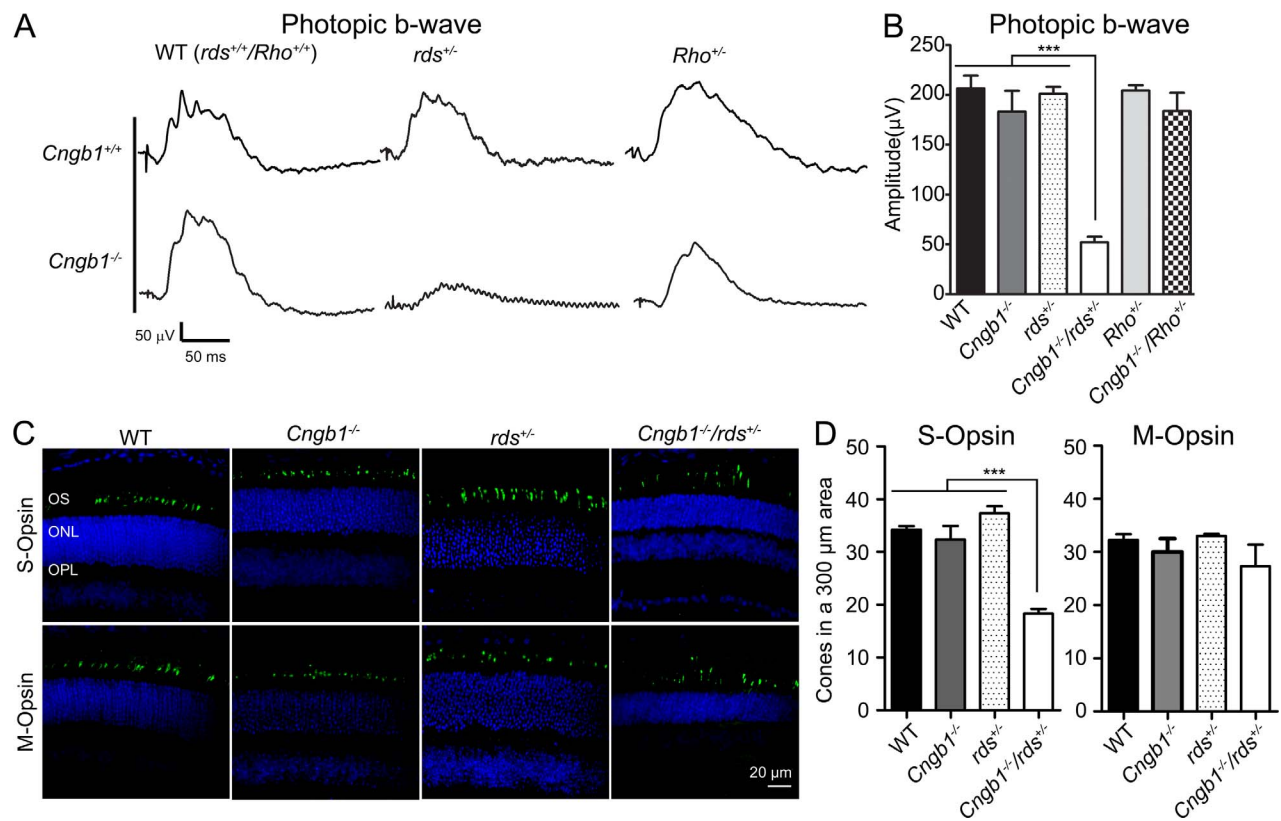


FIGURE 6. Cone function is significantly reduced in the *Cngb1*^{-/-}/*rds*^{+/-} retina. Photopic ERGs were recorded from WT, *Cngb1*^{-/-}, *rds*^{+/-}, *Cngb1*^{-/-}/*rds*^{+/-}, *rbo*^{+/-}, and *Cngb1*^{-/-}/*Rho*^{+/-} at P30. (A) Representative waveforms; (B) plots of the mean maximum photopic b-wave amplitude. *n* = 4 to 7 mice per genotype (**P* < 0.05, ***P* < 0.01, and ****P* < 0.001 by 1-way ANOVA with Bonferroni's post hoc comparison). (C) Paraffin-embedded retinal sections from P30 animals were labeled with anti S-opsin (green, top) and anti-M-opsin (green, bottom) and were all counterstained with DAPI (blue). Scale bar: 20 µm. OS, outer segment; ONL, outer nuclear layer; OPL, outer plexiform layer. (D) Cells positive for cone opsins were counted in a 300-µm region of the central retina either inferior (S-opsin-positive cells) or superior (M-opsin-positive cells) of the optic nerve. Plotted are means ± SEM.

support OS structure and function. Recent work showed that RDS can bind rhodopsin and suggested that a complex composed of CNGB1a, RDS, and rhodopsin may play a structural role in anchoring the rim to the plasma membrane (via RDS-CNGB1a interactions), and a functional role ensuring that proteins are properly localized for optimal phototransduction.¹⁹ When combined with other work showing that CNGB1a/GARP interactions with phosphodiesterase 6 may provide a role for GARP in cGMP turnover,^{17,50-52} these observations suggest that RDS may organize the rim region into a hotspot area or environment for highly regulated phototransduction. This hypothesis is consistent with our results here showing that CNGB1a and RDS can act additively, exacerbating RDS haploinsufficiency, and resulting in (1) severely decreased rod function in *Cngb1*^{-/-}/*rds*^{+/-} versus *Cngb1*^{-/-} or *rds*^{+/-} and (2) modest additional reductions in the thickness of the OS layer and the ONL in the *Cngb1*^{-/-}/*rds*^{+/-} versus the *rds*^{+/-} and *Cngb1*^{-/-}. Critically, however, these additive effects occur without any difference in rod ultrastructure in *Cngb1*^{-/-}/*rds*^{+/-} versus *rds*^{+/-}. This suggests that defects in rod function and overall retinal structure cannot be completely attributed to a role for CNGB1/RDS interactions in maintaining rim structure, but rather that these interactions also organize a functional environment critical for proper signal transduction. This role for RDS as an interactor/organizer of many proteins (i.e., not just ROM-1) is consistent with the observation that RDS also interacts with rhodopsin¹⁹ as well as the known broader role of tetraspanins, which often act as

organizers of membrane domains containing a wide variety of different proteins.⁵³

An interesting outcome from our work is that cone ERG function is significantly reduced in the *Cngb1*^{-/-}/*rds*^{+/-} compared to controls. *Cngb1*^{-/-} is expressed only in rods, and cone function in *Cngb1*^{-/-} animals is normal at P30⁴⁸ and starts decreasing only later, likely a secondary phenomenon due to rod loss. Similarly, while RDS is expressed in rods and cones, cones can better tolerate reduced RDS levels than rods, so cone function in the *rds*^{+/-} is also preserved until approximately 4 months of age.²³ Yet here we see cone degeneration and a dramatic reduction in cone function in *Cngb1*^{-/-}/*rds*^{+/-} as early as P30. This likely represents a rapid acceleration of RDS haploinsufficiency in cones; however, why elimination of CNGB1 in rods should accelerate RDS-associated cone degeneration is not clear. This cone phenotype is not completely due to overt rod loss since ONL thickness is only mildly affected in the *Cngb1*^{-/-}/*rds*^{+/-} versus the *rds*^{+/-}. There may be several underlying causes, including overall alterations in retinal homeostasis, altered secretion of signaling factors from rods needed for cone health, or alterations in other cell types such as horizontal cells and retinal glia that interact with both rods and cones. Further exploration of the mechanisms underlying this cone defect are of great interest given the proliferation of retinal disease wherein secondary cone loss following rod-specific defects leads to worsened patient visual outcomes.

Outer segment trafficking has recently been a field of particular interest. The trafficking pathways for rhodopsin

have been extensively studied,⁵⁴ and RDS and rhodopsin are thought to traffic separately.⁵⁵ Recent work has shown that in contrast to rhodopsin, the majority of RDS does not traffic through the trans-Golgi, but uses an unconventional secretory pathway during OS targeting.^{56,57} Little is known about the regulation of CNGB1a/GARP1/2 trafficking; however, recent work from Goldberg's group¹⁸ shows that RDS/CNGB1a interactions first occur in the inner segment, raising the intriguing possibility that CNGB1a may traffic with RDS. However, whether the CNGB1a would traffic with conventionally or unconventionally processed RDS remains to be further explored. Here we find that in general, trafficking of RDS, ROM-1, and rhodopsin was not affected by *Cngb1* ablation. However, the reverse is more difficult to assess. The presence of a clear region of CNGB1a/GARP1/2 immunoreactivity in the distal inner segment region, likely inside the small abnormally formed OS nubs, suggests that overall, CNGB1a/GARP1/2 targeting is not affected by elimination of rhodopsin; however, we cannot assess the role of RDS in CNGB1a/GARP1/2 trafficking because CNGB1a/GARP1/2 are not detectable in *rds*^{-/-} mice.⁴⁷ Thus, it is not possible to differentiate whether CNGB1a/GARP1/2 trafficking to the OS requires RDS, whether CNGB1a protein stability requires RDS, or whether CNGB1a trafficking/stability require the RDS-mediated assembly of OSs.

Interestingly, in some cases eliminating the CNGB1 channel can be beneficial in preventing or retarding retinal degeneration. For example, the removal of *Cngb1* significantly rescued the rapid degenerative phenotypes in the *rd1* mouse.⁵⁸ Degeneration in the *rd1* was hypothesized to be tied to observed elevated cGMP levels.⁵⁹ However, the removal of CNG channels led to rescue of rod photoreceptors without ameliorating cGMP levels,⁵⁸ suggesting that removing cGMP-mediated signaling was beneficial rather than removing cGMP per se. As a parallel, eliminating RDS in the *rd1* retina (*rds*^{-/-}/*Pde6b*^{rd1/rd1}) also delayed retinal degeneration regardless of the massive accumulation of cGMP.⁶⁰ Our observation that CNGB1a levels are drastically reduced in the *rds*^{-/-} suggests that attenuation of *rd1*-associated retinal degeneration in the *rd1 rds* double knockout is likely due to an elimination of the CNG channel/CNGB1a rather than to the loss of RDS per se.

In conclusion, we here present data showing that elimination of CNGB1 exacerbates RDS-associated functional but not structural haploinsufficiency. These observations suggest that RDS/CNGB1 interactions have a role in OS function in addition to structure and are consistent with the hypothesis that RDS functions as a component of a multiprotein plasma membrane-rim-disc complex critical for OSs.

Acknowledgments

The authors thank Barb Nagel and Jamie Watson for their excellent technical assistance. We also thank Neeraj Agarwal, Janice Lem, and Robert Molday for the provision of reagents/animals as indicated in the text.

Supported by National Institutes of Health (NIH) Grant R01EY010609 (MIN), by the Oklahoma Center for the Advancement of Science and Technology (SMC), and by NIH Grants R01EY018143-06 and P30EY003039-35 and the Vision Science Research Center (SJP).

Disclosure: **D. Chakraborty**, None; **S.M. Conley**, None; **S.J. Pittler**, None; **M.I. Naash**, None

References

- Dryja TP, McGee TL, Reichel E, et al. A point mutation of the rhodopsin gene in one form of retinitis pigmentosa. *Nature*. 1990;343:364-366.
- Skiba NP, Spencer WJ, Salinas RY, Lieu EC, Thompson JW, Arshavsky VY. Proteomic identification of unique photoreceptor disc components reveals the presence of PRCD, a protein linked to retinal degeneration. *J Proteome Res*. 2013;12:3010-3018.
- Kwok MC, Holopainen JM, Molday LL, Foster LJ, Molday RS. Proteomics of photoreceptor outer segments identifies a subset of SNARE and Rab proteins implicated in membrane vesicle trafficking and fusion. *Mol Cell Proteomics*. 2008;7:1053-1066.
- Harosi FI. Absorption spectra and linear dichroism of some amphibian photoreceptors. *J Gen Physiol*. 1975;66:357-382.
- Liebman PA, Entine G. Visual pigments of frog and tadpole (*Rana pipiens*). *Vision Res*. 1968;8:761-775.
- Humphries MM, Rancourt D, Farrar GJ, et al. Retinopathy induced in mice by targeted disruption of the rhodopsin gene. *Nat Genet*. 1997;15:216-219.
- Lem J, Krasnoperova NV, Calvert PD, et al. Morphological, physiological, and biochemical changes in rhodopsin knockout mice. *Proc Natl Acad Sci U S A*. 1999;96:736-741.
- Chakraborty D, Conley SM, Al-Ubaidi MR, Naash MI. Initiation of rod outer segment disc formation requires RDS. *PLoS One*. 2014;9:e98939.
- Liang Y, Fotiadis D, Maeda T, et al. Rhodopsin signaling and organization in heterozygote rhodopsin knockout mice. *J Biol Chem*. 2004;279:48189-48196.
- Makino CL, Wen XH, Michaud NA, et al. Rhodopsin expression level affects rod outer segment morphology and photoreceptor kinetics. *PLoS One*. 2012;7:e37832.
- Molday RS, Hicks D, Molday L. Peripherin. A rim-specific membrane protein of rod outer segment discs. *Invest Ophthalmol Vis Sci*. 1987;28:50-61.
- Bascom RA, Manara S, Collins L, Molday RS, Kalnins VI, McInnes RR. Cloning of the cDNA for a novel photoreceptor membrane protein (rom-1) identifies a disk rim protein family implicated in human retinopathies. *Neuron*. 1992;8:1171-1184.
- Kajiwaru K, Hahn LB, Mukai S, Travis GH, Berson EL, Dryja TP. Mutations in the human retinal degeneration slow gene in autosomal dominant retinitis pigmentosa. *Nature*. 1991;354:480-483.
- Wells J, Wroblewski J, Keen J, et al. Mutations in the human retinal degeneration slow (RDS) gene can cause either retinitis pigmentosa or macular dystrophy. *Nat Genet*. 1993;3:213-218.
- Boesze-Battaglia K, Goldberg AF, Dispoto J, Katragadda M, Cesarone G, Albert AD. A soluble peripherin/Rds C-terminal polypeptide promotes membrane fusion and changes conformation upon membrane association. *Exp Eye Res*. 2003;77:505-514.
- Khattree N, Ritter LM, Goldberg AF. Membrane curvature generation by a C-terminal amphipathic helix in peripherin-2/ rds, a tetraspanin required for photoreceptor sensory cilium morphogenesis. *J Cell Sci*. 2013;126:4659-4670.
- Poetsch A, Molday LL, Molday RS. The cGMP-gated channel and related glutamic acid-rich proteins interact with peripherin-2 at the rim region of rod photoreceptor disc membranes. *J Biol Chem*. 2001;276:48009-48016.
- Ritter LM, Khattree N, Tam B, Moritz OL, Schmitz F, Goldberg AF. In situ visualization of protein interactions in sensory neurons: glutamic acid-rich proteins (GARPs) play differential roles for photoreceptor outer segment scaffolding. *J Neurosci*. 2011;31:11231-11243.
- Becirovic E, Nguyen ON, Pappas C, et al. Peripherin-2 couples rhodopsin to the CNG channel in outer segments of rod photoreceptors. *Hum Mol Genet*. 2014;23:5989-5997.

20. Jansen HG, Sanyal S. Development and degeneration of retina in rds mutant mice: electron microscopy. *J Comp Neurol*. 1984;224:71-84.
21. Sanyal S, Jansen HG. Absence of receptor outer segments in the retina of rds mutant mice. *Neurosci Lett*. 1981;21:23-26.
22. Sanyal S, Zeilmaker GH. Development and degeneration of retina in rds mutant mice: light and electron microscopic observations in experimental chimaeras. *Exp Eye Res*. 1984;39:231-246.
23. Cheng T, Peachey NS, Li S, Goto Y, Cao Y, Naash MI. The effect of peripherin/rds haploinsufficiency on rod and cone photoreceptors. *J Neurosci*. 1997;17:8118-8128.
24. Boon CJ, den Hollander AI, Hoyng CB, Cremers FP, Klevering BJ, Keunen JE. The spectrum of retinal dystrophies caused by mutations in the peripherin/RDS gene. *Prog Retin Eye Res*. 2008;27:213-235.
25. Zhong H, Molday LL, Molday RS, Yau KW. The heteromeric cyclic nucleotide-gated channel adopts a 3A:1B stoichiometry. *Nature*. 2002;420:193-198.
26. Saqib MA, Nikopoulos K, Ullah E, et al. Homozygosity mapping reveals novel and known mutations in Pakistani families with inherited retinal dystrophies. *Sci Rep*. 2015;5:9965.
27. Maria M, Ajmal M, Azam M, et al. Homozygosity mapping and targeted sanger sequencing reveal genetic defects underlying inherited retinal disease in families from Pakistan. *PLoS One*. 2015;10:e0119806.
28. Bocquet B, Marzouka NA, Hebrard M, et al. Homozygosity mapping in autosomal recessive retinitis pigmentosa families detects novel mutations. *Mol Vis*. 2013;19:2487-2500.
29. Nishiguchi KM, Tearle RG, Liu YP, et al. Whole genome sequencing in patients with retinitis pigmentosa reveals pathogenic DNA structural changes and NEK2 as a new disease gene. *Proc Natl Acad Sci U S A*. 2013;110:16139-16144.
30. Schorderet DF, Iouranova A, Favez T, Tiab L, Escher P, IROme, a new high-throughput molecular tool for the diagnosis of inherited retinal dystrophies. *Biomed Res Int*. 2013;2013:198089.
31. Becirovic E, Nakova K, Hammelmann V, Hennel R, Biel M, Michalakis S. The retinitis pigmentosa mutation c.3444+1G>A in CNGB1 results in skipping of exon 32. *PLoS One*. 2010;5:e8969.
32. Kondo H, Qin M, Mizota A, et al. A homozygosity-based search for mutations in patients with autosomal recessive retinitis pigmentosa, using microsatellite markers. *Invest Ophthalmol Vis Sci*. 2004;45:4433-4439.
33. Bareil C, Hamel CP, Delague V, Arnaud B, Demaille J, Claustres M. Segregation of a mutation in CNGB1 encoding the beta-subunit of the rod cGMP-gated channel in a family with autosomal recessive retinitis pigmentosa. *Hum Genet*. 2001;108:328-334.
34. Zhang Y, Molday LL, Molday RS, et al. Knockout of GARPs and the beta-subunit of the rod cGMP-gated channel disrupts disk morphogenesis and rod outer segment structural integrity. *J Cell Sci*. 2009;122:1192-1200.
35. Ardell MD, Bedsole DL, Schoborg RV, Pittler SJ. Genomic organization of the human rod photoreceptor cGMP-gated cation channel beta-subunit gene. *Gene*. 2000;245:311-318.
36. Colville CA, Molday RS. Primary structure and expression of the human beta-subunit and related proteins of the rod photoreceptor cGMP-gated channel. *J Biol Chem*. 1996;271:32968-32974.
37. Gilliam JC, Chang JT, Sandoval IM, et al. Three-dimensional architecture of the rod sensory cilium and its disruption in retinal neurodegeneration. *Cell*. 2012;151:1029-1041.
38. Chakraborty D, Ding XQ, Conley SM, Fliesler SJ, Naash MI. Differential requirements for retinal degeneration slow intermolecular disulfide-linked oligomerization in rods versus cones. *Hum Mol Genet*. 2009;18:797-808.
39. Chakraborty D, Ding XQ, Fliesler SJ, Naash MI. Outer segment oligomerization of Rds: evidence from mouse models and subcellular fractionation. *Biochemistry (Mosc)*. 2008;47:1144-1156.
40. Chakraborty D, Conley SM, Stuck MW, Naash MI. Differences in RDS trafficking, assembly and function in cones versus rods: insights from studies of C150S-RDS. *Hum Mol Genet*. 2010;19:4799-4812.
41. Conley SM, Stuck MW, Burnett JL, et al. Insights into the mechanisms of macular degeneration associated with the R172W mutation in RDS. *Hum Mol Genet*. 2014;23:3102-3114.
42. Stuck MW, Conley SM, Naash MI. The Y141C knockin mutation in RDS leads to complex phenotypes in the mouse. *Hum Mol Genet*. 2014;23:6260-6274.
43. MacKenzie D, Arendt A, Hargrave P, McDowell JH, Molday RS. Localization of binding sites for carboxyl terminal specific anti-rhodopsin monoclonal antibodies using synthetic peptides. *Biochemistry (Mosc)*. 1984;23:6544-6549.
44. Conley SM, Al-Ubaidi MR, Han Z, Naash MI. Rim formation is not a prerequisite for distribution of cone photoreceptor outer segment proteins. *FASEB J*. 2014;28:3468-3479.
45. Farjo R, Skaggs JS, Nagel BA, et al. Retention of function without normal disc morphogenesis occurs in cone but not rod photoreceptors. *J Cell Biol*. 2006;173:59-68.
46. Stricker HM, Ding XQ, Quiambao A, Fliesler SJ, Naash MI. The Cys214->Ser mutation in peripherin/rds causes a loss-of-function phenotype in transgenic mice. *Biochem J*. 2005;388:605-613.
47. Chakraborty D, Conley SM, DeRamus ML, Pittler SJ, Naash MI. Varying the GARP2-to-RDS ratio leads to defects in rim formation and rod and cone function. *Invest Ophthalmol Vis Sci*. 2015;56:8187-8198.
48. Zhang Y, Rubin GR, Fineberg N, et al. Age-related changes in *Cngb1-X1* knockout mice: prolonged cone survival. *Doc Ophthalmol*. 2012;124:163-175.
49. Huttel S, Michalakis S, Seeliger M, et al. Impaired channel targeting and retinal degeneration in mice lacking the cyclic nucleotide-gated channel subunit CNGB1. *J Neurosci*. 2005;25:130-138.
50. Korschen HG, Beyermann M, Muller F, et al. Interaction of glutamic-acid-rich proteins with the cGMP signalling pathway in rod photoreceptors. *Nature*. 1999;400:761-766.
51. Sarfare S, McKeown AS, Messinger J, et al. Overexpression of rod photoreceptor glutamic acid rich protein 2 (GARP2) increases gain and slows recovery in mouse retina. *Cell Commun Signal*. 2014;12:67.
52. Michalakis S, Zong X, Becirovic E, et al. The glutamic acid-rich protein is a gating inhibitor of cyclic nucleotide-gated channels. *J Neurosci*. 2011;31:133-141.
53. Conley SM, Stuck MW, Naash MI. Structural and functional relationships between photoreceptor tetraspanins and other superfamily members. *Cell Mol Life Sci*. 2012;69:1035-1047.
54. Wang J, Deretic D. Molecular complexes that direct rhodopsin transport to primary cilia. *Prog Retin Eye Res*. 2014;38:1-19.
55. Fariss RN, Molday RS, Fisher SK, Matsumoto B. Evidence from normal and degenerating photoreceptors that two outer segment integral membrane proteins have separate transport pathways. *J Comp Neurol*. 1997;387:148-156.
56. Zulliger R, Conley SM, Mwoyosvi ML, Stuck MW, Azadi S, Naash MI. SNAREs interact with retinal degeneration slow and rod outer segment membrane protein-1 during conventional

- and unconventional outer segment targeting. *PLoS One*. 2015; 10:e0138508.
57. Tian G, Ropelewski P, Nemet I, Lee R, Lodowski KH, Imanishi Y. An unconventional secretory pathway mediates the cilia targeting of peripherin/rds. *J Neurosci*. 2014;34:992-1006.
 58. Paquet-Durand F, Beck S, Michalakis S, et al. A key role for cyclic nucleotide gated (CNG) channels in cGMP-related retinitis pigmentosa. *Hum Mol Genet*. 2011;20:941-947.
 59. Lolley RN, Farber DB, Rayborn ME, Hollyfield JG. Cyclic GMP accumulation causes degeneration of photoreceptor cells: simulation of an inherited disease. *Science*. 1977;196:664-666.
 60. Fletcher RT, Sanyal S, Krishna G, Aguirre G, Chader GJ. Genetic expression of cyclic GMP phosphodiesterase activity defines abnormal photoreceptor differentiation in neurological mutants of inherited retinal degeneration. *J Neurochem*. 1986;46: 1240-1245.